Available online at www.sciencedirect.com
ScienceDirect
Journal of the European Ceramic Society 29 (2009) 207–221
www.elsevier.com/locate/jeurceramsoc

Transmission physics and consequences for materials selection, manufacturing, and applications

Andreas Krell *, Thomas Hutzler, Jens Klimke

Fraunhofer Institut für Keramische Technologien und Systeme (IKTS), Winterbergstr. 28, D-01277 Dresden, Germany

Available online 23 May 2008

Abstract

The differences of translucency and transparency request special conditions for a right photographic presentation and for correct transmission measurements. These differences also influence the materials design of products because of the effect of thickness. Prerequisites of a clear transparency of ceramics are derived for inherent materials properties and for the microstructures starting from a comparison of amorphous, single crystalline and sintered polycrystalline transparent materials. Manufacturing principles differ for transparent cubic and non-cubic ceramics; they have to respond to frequently extreme microstructural requirements, to the available basis of raw materials, and to individual shape, size, and property objectives of applications. A range of present and future applications is addressed and evaluated as governed by, on the one hand, a sensible balance of stringent needs in different fields of the industry with, on the other hand, the costs of development and manufacture.

Keywords: Transparent ceramics; Translucent ceramics; Light transmission; Defect-free processing; Alumina Al_2O_3; Spinel $MgO{\cdot}Al_2O_3$; AlON; Yttria Y_2O_3; Garnet YAG; Zirconia ZrO_2; Lighting; IR emitters; Laser ceramics; Lenses; Microlithography; Tools; Dental ceramics; Gemstones; Armour

1. Transparent vs. translucent performance

1.1. Demonstration of differences

Some languages (as German) give rise to misunderstandings when, e.g. tracing paper is called "transparent paper" (in disagreement to its only *translucent* appearance). It has, therefore, to be emphasised that in the vocabulary of science and technology components are called *transparent* only if they provide clear images with a larger distance between the object and the transparent window. Obviously, such "clear" images need a way of light propagation where most of the intensity of the beams remains in-line and is not scattered.

With this need of a high *in-line* transmission there are two important consequences for characterisation approaches intended to distinguish transparent from translucent materials.

Frequently, a first qualitative evidence of transparency is obtained by simple observation. Here, a right approach needs a *larger distance* between the background and the window (Fig. 1a). On the contrary, direct placing of windows on a printed matter removes all characteristic differences and provides similarly "clear" images with *both* translucent and transparent materials (Fig. 1b). It was repeatedly emphasised that such "evidence" does, therefore, *not* provide *the least* information about the transparency of a material.[1] Nevertheless, numerous publications are still accepted around the globe with wrong figures like Fig. 1b pretending erroneously that this demonstration could inform about an achieved transparent character.

Similar misleading and wrong conclusions on "transparency" (= provided by unscattered "in-line" light) are sometimes derived from transmission *measurements* if optical devices are used with an unspecified aperture (half of opening angle): if on transmission through a medium only some part of the beam remains "in-line" in its original direction with other parts of the intensity scattered aside (Fig. 2b) it is obvious that with an opening angle of, e.g. 5° instead of 0.5° significant scattered amounts will contribute to an unspecified "in-line" record (10-fold angle means a 100-fold recording area for such "in-line" data). Unfortunately, records of poorly defined "in-line" or "linear" transmissions obtained by commercial photospectrometers with apertures in the range of 3–5°[2] are quite common. In order to exclude the scattered amounts from the measured intensity it is, therefore, important to measure a "real" in-line transmission by using an aperture close to zero. In fact, a zero aperture is impractical and technical opening angles are very small but *finite*. Without a unified international standard, leading manu-

* Corresponding author.
E-mail address: Andreas.Krell@ikts.fraunhofer.de (A. Krell).

0955-2219/$ – see front matter © 2008 Elsevier Ltd. All rights reserved.
doi:10.1016/j.jeurceramsoc.2008.03.025

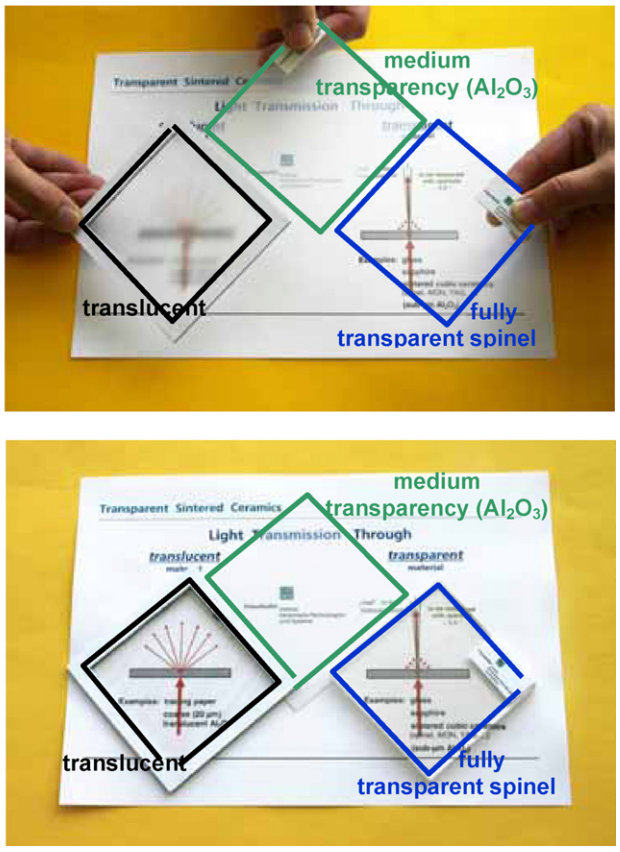

Fig. 1. Comparison of 0.06 mm thin translucent organic material, sintered window of sub-μm Al_2O_3 (thickness 0.8 mm, real in-line transmission ~60%), and 6 mm thick almost fully transparent spinel. The characteristic differences of transmission are clearly demonstrated by (a), the wrong positioning in (b) does not provide any information about the degree of transparency: without a larger distance between object and window there is no apparent difference of *translucent* (here: extremely thin!) and *transparent* materials.

facturers of ceramic discharge lamps as Philips and NGK Spark Plug have published investigations that use a "real in-line transmission" RIT obtained with an aperture of about 0.5°,[2,3] and it is recommended to join this approach.

An alternative option of transparency measurement is the quantitative determination of the image resolution of a black/white bar lattice as it is common in optics (→ measurement of the modulation transmission function MTF).[4,5]

1.2. Maximum transmission and thickness effect

Another technically important issue is thickness. Without scattering or absorption losses, the theoretical maximum of transmission is 100% minus reflection on both surfaces of a window. At normal incidence, the reflection R_1 on one surface is governed by the refractive index n as

$$R_1 = \left\{\frac{n-1}{n+1}\right\}^2, \tag{1a}$$

and the total reflection loss (including multiple reflection) is

$$R_2 = \frac{2R_1}{1+R_1}. \tag{1b}$$

Thus, the theoretical limit is

$$T_{th} = (1-R_2) = \frac{2n}{n^2+1}. \tag{2}$$

Even a high "real" transmission of, e.g. 60% of T_{th} measured for a given thickness means 40% losses by scatter or absorption *over this thickness*, and these losses increase with growing thickness (Fig. 2b→a). Hence, Fig. 2a and b demonstrates that any statement like "*Transmission* (at thickness = *x* mm) < *theoretical maximum*" is identical with a significant impact of the *thickness* on the transmission of this material in a way that beyond some critical thickness it is subject to a translucent only performance.[6] Fig. 3 shows this transition for a sintered Al_2O_3 ceramic with sub-μm grain size.

Therefore, an expression like "*fully* transparent" should be preserved for materials only which exhibit clear transparency independent of the thickness – which needs a "real" in-line transmission RIT (measured, e.g. at 2 mm thickness) close to the theoretical maximum (= materials that do not cause losses by absorption or scatter – Fig. 2c).

As a consequence, most ceramics are not generally *transparent* or *translucent*, this characterisation needs the reference to some thickness. As outlined above the thickness effect is most important for ceramics which due to scattering losses exhibit a larger difference between their real in-line transmission (e.g. at a thickness of 1–2 mm) and the theoretical maximum.

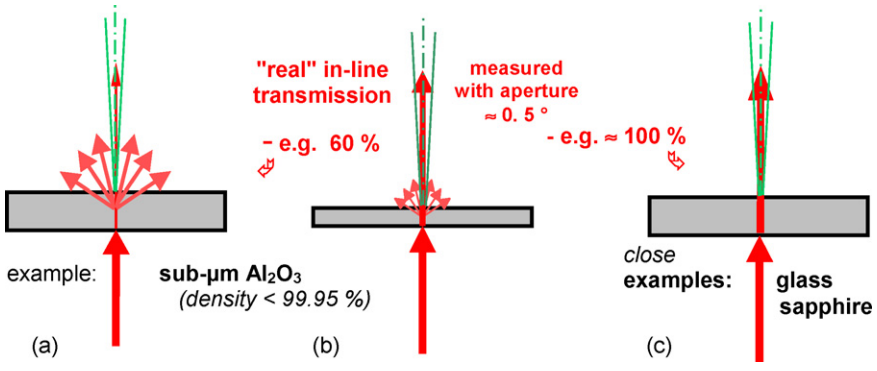

Fig. 2. Reliable determination of a "real" in-line transmission enabled by narrow measuring aperture (b). Scattering or absorption losses reduce the in-line transmission to <100% and give rise to a significant thickness effect (b→a). This thickness effect disappears when the transmission approaches the theoretical maximum (c).

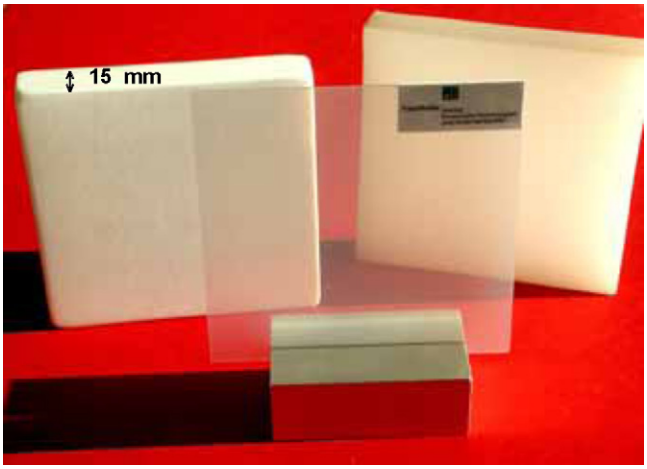

Fig. 3. High transparency of sintered sub-μm Al_2O_3 (relative density >99.95%) with real in-line transmission ~60 % at 0.8 mm thickness (central sample) whereas the identical material is translucent at larger thickness (right); it becomes opaque (white) when the residual porosity is >0.1% (left).

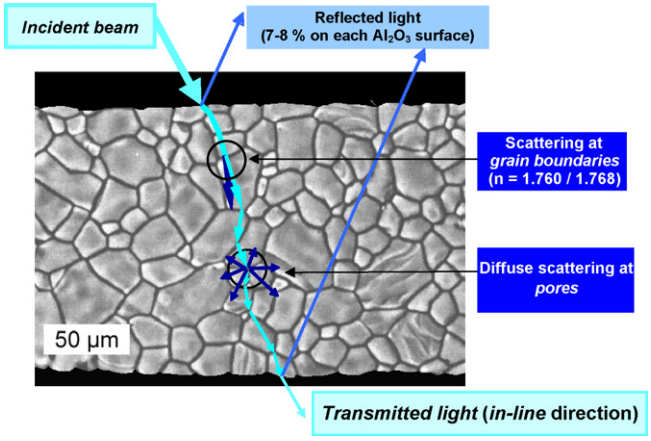

Fig. 4. Light transmission through a polycrystalline isolator (example: translucent coarse Al_2O_3 microstructure). Losses of the original intensity are caused beyond absorption by (i) reflection on both surfaces, (ii) diffuse scattering at pores and (iii) scattering by birefringent splitting (the latter is active in *non-cubic* [= optically non-isotropic] crystallites only).

2. Transmission through sintered polycrystals—consequences for materials selection and microstructural design

2.1. Inherent property requirements, scattering by second phases, grain size and wavelength effects

Materials selection for transparent components starts with the consideration that a minimum of light *absorption* means least interaction of the electromagnetic wave with the material of the "window". A free electron gas as in metals will, obviously, not contribute to a behaviour like this, and isolators are clearly preferred.

Within this frame of isolators *scattering losses* are on a minimum when the material is optically *homogeneous* (no second phases with different n that give rise to light scattering) and *isotropic* (no birefringence). With this background it is well understandable that glass is the most common among the traditional transparent materials. Its easy, almost unlimited shapeability (e.g. by the glass blower) is, however, also its most limiting shortcoming: this transparent material is stable at rather low temperatures only, and even at ambient conditions it does not exhibit high mechanical or corrosive parameters.

Similarly well known for ages are *single crystalline* transparent "ceramic" isolators—the natural gemstones. They are provided by a number of growth processes for use in industrial applications (e.g. for lasers or in mechanical watches), but two difficulties hinder a broader use: the expensive and limited to simple shapes manufacture, and in the case of non-cubic crystals specific disadvantages in mechanical and optical properties compared with isotropic polycrystalline materials.

Most of such shortcomings can be overcome by *polycrystalline* (sintered) transparent materials. On light transmission through polycrystalline ceramics, however, additional mechanisms have to be considered compared with the processes in more homogeneous materials. Scattering losses decrease the in-line transmission depending on the microstructure (Fig. 4):

1. By diffuse scattering at second phases as pores or microstructural components with different refractive index (similarly relevant in *all* transparent materials), and
2. in *non-cubic* ceramics by additional scattering caused by birefringent splitting of the beam at grain boundaries.[2]

Clear transparency is observed through a thickness of about 1 mm when small scattering losses enable a real in-line transmission ≥0.65–0.70 of the theoretical limit[1]; higher values are, of course, beneficial.

Obviously, the critically addressed above thickness effect has to be expected first of all for ceramics where both mechanisms of Fig. 4 contribute to losses. This is unavoidable for all *non-cubic* crystals[a]. Sintered corundum (Al_2O_3) is the technically most important example of this group of ceramics that with a *fixed microstructure* may turn transparent or translucent depending on thickness. Extreme technological challenges result for the manufacture of such ceramics where even 1 mm thin windows exhibit good transparency only if scattering losses (caused by birefringence) are minimized by keeping the grain size in the far sub-μm range[b].[1] Depending on $\Delta n/n$[c] a physical model using Mie's theory[2] has described these influences of grain size $2r$, wavelength λ_m (in the medium; $\lambda_m = \lambda_0/n$), and thickness d on the real in-line transmission RIT of a completely dense microstructure by

$$\mathrm{RIT} = T_{th} \exp\left\{-3\pi^2 \frac{\Delta n^2 r d}{n^2 \lambda^2}\right\} \quad (3)$$

with the theoretical maximum $T_{th} = 2n/(n^2+1)$ as introduced above by Eq. (2).

[a] The smaller effect of *intrinsic birefringence* of cubic crystals will be addressed below in Section 5.3.2.

[b] For some applications highly transparent *single* crystals can be a solution but are expensive and associated with shortcomings in manufacture and properties.

[c] Ratio of refractive index difference for polarization perpendicular and parallel to c-axis to the average index n.

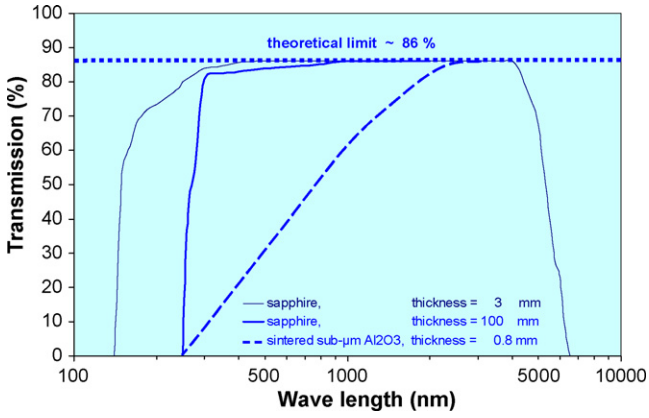

Fig. 5. Typical transmission curves of poly- and single-crystalline corundum. The strong wavelength effect for sintered alumina is associated with its birefringent character, *cubic* polycrystalline ceramics do not exhibit this effect (cp. discussion of Fig. 4 above). Note that close to an absorption edge thickness becomes very important (shown here exemplarily near the UV edge of sapphire).

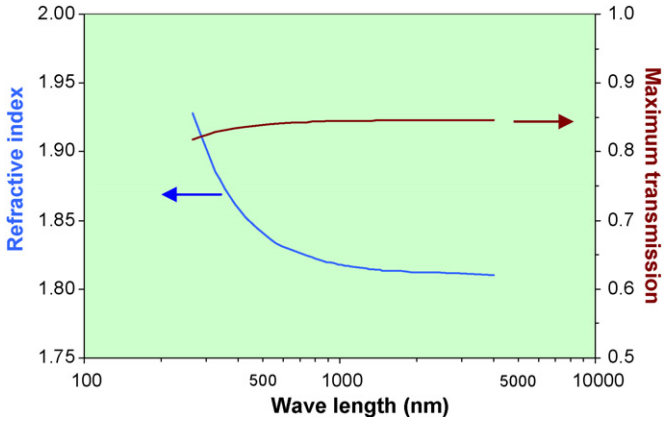

Fig. 6. Wavelength dependence of the refractive index of single crystalline yttria alumina garnet (YAG) and resulting (calculated by Eq. (2)) theoretical transmission.

The most important practical message of Eq. (3) is the equivalence of the two influences of grain size $2r$ and of wavelength λ:

- Scattering losses associated with birefringence are the smaller and transmission RIT increases the more the lesser the wave package is able to distinguish individual crystals, i.e. the smaller the grain size is. Typically, the grain size of highly dense sintered Al_2O_3 has to be about 0.5 μm for RIT ≈60–65% at $\lambda = 640$ nm and $d = 1$ mm.
- On the other hand, smaller grain sizes at a fixed wavelength have the same physical meaning as increased wavelengths at fixed grain size (cp. Eq. (3)). Really, Fig. 5 shows an increasing transmission through a sintered sub-μm Al_2O_3 grade from the UV up to the IR range[7]—in contrast to the behaviour of *single* crystalline alumina which does not suffer increasing birefringent scattering losses at shorter wavelengths and shows, therefore, an approximately constant transmission.

Of course, both single and polycrystalline alumina exhibit a similar absorption edge at very short UV wavelengths (Fig. 5) which give rise to the transition of valence electrons into orbitals with an increased state of energy. This photoexcitation of electrons and the associated absorption start when UV light is available with a wavelength that corresponds to a defined energy shift and when the electronic transition in the solid body is allowed by the quantum mechanical rules.

On the IR side of the spectrum, radiation does not exhibit enough energy to induce electronic transitions as with UV. Here the decreasing transmission (increasing absorption) is associated with small energy differences in the vibrational (and rotational) states of molecules, amorphous networks or lattices (phonon modes).

In the UV range an additional effect arises from the increasing dependence of the refractive index on the wavelength (Fig. 6): reflection increases at shorter wavelengths and reduces the theoretical maximum T_{th} of transmission according to Eq. (2). With Fig. 6 it is, however, clear that this effect is small compared with the consequence of UV absorption which for the shown example of YAG ends transmission at $\lambda \leq 280$ nm.

Technically more important are some direct consequences of dispersion, i.e. of the dependence of the refractive index n on wavelength λ, described empirically, e.g. by

$$n(\lambda)^2 = A_0 + A_1\lambda^2 + A_2\lambda^{-2} + A_3\lambda^{-4} + A_4\lambda^{-6} + A_5\lambda^{-8} + \ldots \quad (4)$$

(unit of λ is μm; the coefficients A_0 to A_5 are given by optical handbooks). With the increasing influence of the wavelength at shorter values (Fig. 6), the *degree* of dispersion is different in the different ranges. For visible light the dispersion of optical glasses is commonly described by an Abbé number:

$$v_d = \frac{n_d - 1}{n_F - n_C} \quad (5a)$$

where subscripts d, F and C identify the parameters as values at wavelengths of the corresponding Fraunhofer lines d (587.56 nm), F (486.13 nm), and C (656.28 nm); an analogous definition uses the index at the D-line (589.2 nm) instead of n_d.

Whereas a high index n is important, e.g. for the design of small lenses, high Abbé values are beneficial as characteristic for materials which exhibit *small variations* of n at high n values. However, in the traditional glass diagram (Abbé diagram, Fig. 7) a high index is commonly accompanied by *decreasing* Abbé numbers. Interestingly, the incorporation of *crystalline* materials data into this plot shows that ceramics follow the same general trend at, however, higher n and providing much higher Abbé values for similar n (e.g. when comparing high index glasses at $n \approx 1.6$–1.7 with ceramics of this index).

Since the focal length of lenses depends on the index n, different wavelengths of light are focused on different positions giving rise to fringes of colour around an image. Achromatic doublet lenses combine materials with different dispersion characteristics in order to correct this chromatic aberration. Depending on the technically relevant wavelength zone, a partial dispersion ratio $\theta_{g,F}$ is defined, e.g. for the range between g (435.83 nm)

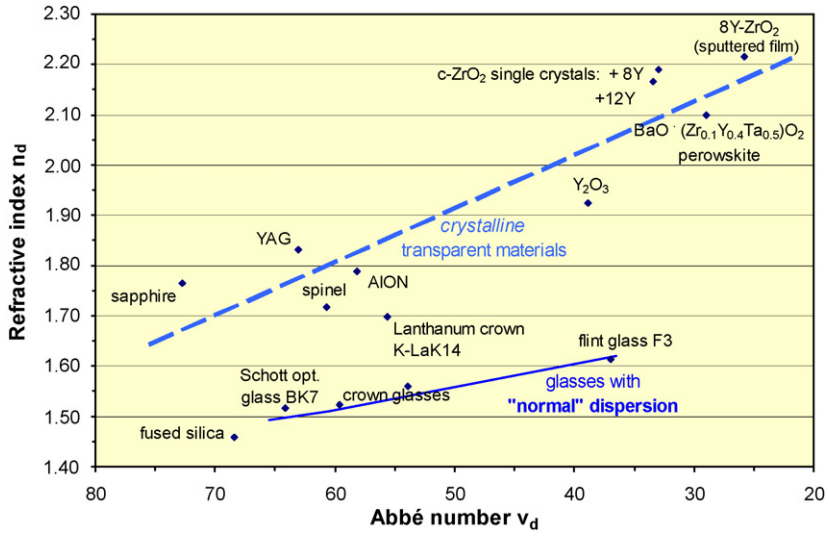

Fig. 7. Abbé diagram: traditional plot of the degree of dispersion (Abbé number v_d) and the refractive index n. According to Abbé, glasses with "normal" dispersion lie along the solid line connecting the points ($v_d = 60.5$, $n_d = 1.511$) and ($v_d = 36.3$, $n_d = 1.620$).

and F lines (486.13 nm) by

$$\theta_{g,F} = \frac{n_g - n_F}{n_F - n_C}, \tag{5b}$$

where again (as in Fig. 7) common optical glasses are positioned close to a linear band (Fig. 8). Recently, materials of high anomalous dispersion with *negative* deviation $\Delta(\theta_{g,F})$ from the linear dependence are required for special optical uses. Such a behaviour has been disclosed for some translucent perowskites with Abbé numbers of about 30,[8] and similar $\Delta(\theta_{g,F})$ are known at higher $v_d \approx 60$, e.g. for magnesia-alumina spinel (whereas other crystalline materials as, e.g. sapphire exhibit *positive* $\Delta(\theta_{g,F})$, i.e. a larger dispersion compared with optical glasses in the g–F range).

2.2. Influences of surface roughness and size effect

With Eq. (3), the absolute transmission cannot amount 100% but is limited to an upper maximum $T_{th} = 2n/(n^2 + 1)$. Therefore, the meaning of an *absolute* real in-line transmission of, e.g. 70% at $\lambda = 600$ nm is rather different when obtained, e.g.

- for sintered cubic ZrO_2 with $n = 2.177$ and $T_{th} = 75.9\%$ where, therefore, the measured result equals a high value of 0.92 T_{th} (=*few* 8% of absorption or scattering losses),
- whereas for sintered Al_2O_3 with $n = 1.765$ the *same absolute* transmission is equivalent to only 0.82 T_{th} (with $T_{th} = 85.8\%$ the measured result means 18% of losses here).

Additionally it has to be kept in mind that $T_{th} = 2n/(n^2 + 1)$ considers the reflection *on theoretically perfect* surfaces. Real reflection on real ceramic windows is affected, however, by the technical roughness which gives rise to additional losses—another mechanism which decreases the real in-line transmission of products or of measured samples depending on the quality of surface preparation and on the measuring approach. Table 1 shows that this effect is in no way negligible but can be handled for measurements in a way that frequently (*not*: always!) results close to maximum are obtained from simply ground (*not* polished!) samples when an immersion liquid is used.

As an example, the last line of Table 1 gives the local scatter of RIT (dominated by the homogeneity of the ceramic, independent of surface preparation and measurement).

An interesting correlation of *technology-dependent* homogeneity and the achieved degree of transparency is revealed by the leap of transmission observed for the 0.6 mm thin sample (where some contribution to this leap originated also from the improved polish). The thickness of this thin disc was not reduced to 0.6 mm by grinding and polishing starting from a same thickness as in the other experiments but the sample was slip-cast with an originally smaller thickness. Obviously, this size effect is the same as known from the strength of ceramics: the manufacture of small scales improves the chances of a defect-free microstructure which is homogeneous over the whole body—resulting in a higher strength (= reduced probability of larger flaws) *and* in a higher transmission (= reduced scattering losses because of reduced population of optical heterogeneities).

3. Guidelines for manufacturing: particle size and homogeneity

Understanding the difficulties associated for optically non-isotropic crystals with $\Delta n \neq 0$ in Eq. (3), the development of transparent ceramics had been focused in early years to *cubic* materials like spinel ($MgO{\cdot}Al_2O_3$).[9] Because the transparency of these first spinel ceramics was insufficient, residual porosity was eliminated in the following decades by higher temperatures while accepting more grain growth (with $\Delta n = 0$ the direct influence of the grain size disappears in Eq. (3)). Unfortunately, the mechanical parameters of known cubic transparent ceramics are generally inferior to (non-cubic) corundum. Additionally, the chance of obtaining highly transparent cubic ceramics (even on

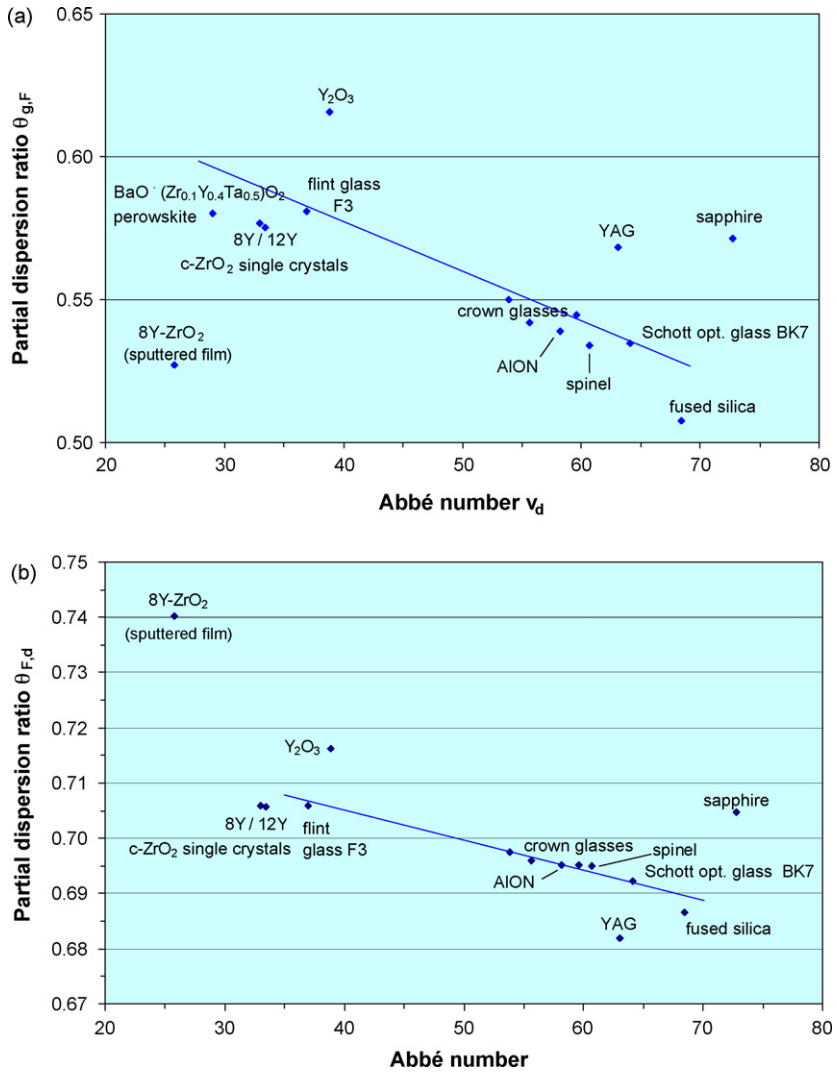

Fig. 8. Partial dispersion ratios (a) $\theta_{g,F}$ (435.83–486.13 nm) and (b) $\theta_{F,d}$ (486.13–587.56 nm) as function of Abbé number; larger deviations from the linear relationship of common optical glasses are addressed as anomalous dispersion. The character of such plots and the individual deviations of transparent ceramics from the line of normal dispersion are different for different wavelength ranges (a and b). Since with Eq. (5b) the position of data is governed by the fourth and fifth digit after the point of n values, these plots are extremely sensible to chemical compositions, resulting dispersion $n(\lambda)$ and the accuracy of n measurements.

tolerating some grain growth) has directed the development of the past 25 years towards *extremely coarse* cubic microstructures up to grain sizes of 50–300 μm[10–12]—accompanied by a further reduction of the mechanical parameters (as an example, the hardness of such coarse transparent spinel is about HV10 = 12 GPa only[13]).

On the other hand, it has to be emphasised that even from the viewpoint of the transparency of cubic polycrystals "unlimited" grain growth is *not* an easily tolerable feature because it is associated with the risk of an inclusion of pores into the growing grains. Then, on further sintering it is very difficult to remove such *intra*granular pores—with

Table 1
Real in-line transmission RIT of slip-cast and hot-isostatically pressed alumina (thickness 0.8–1 mm if not stated otherwise)

Grain size (μm)	Processing	HIP temperature (°C)	RIT_{ground} ($R_A \approx 200$ nm) +*IL*	$RIT_{polished}$ ($R_A = 4$ nm)	$RIT_{polished}$ ($R_A < 4$ nm) 0.6 mm thin sample	$RIT_{polished}$ ($R_A = 4$ nm) +IL
0.38	As-received powder (150 nm)	1170	55.3%	55.8%		**61.7**%
0.34	+Milling	1130	71.1%	66.8%	79.5%	**72.2**%
0.50	+Milling	1250	64.0 ± 1.0%	61.5 ± 0.9%		**66.3** ± 1.4%

All original results (λ = 640 nm, aperture 0.57°) were re-calculated by Eq. (3) for a unified thickness of exactly 0.8 mm. R_a = average surface roughness. +IL = measurement of sample with immersion liquid (di-jodomethane) between two glass plates.

the final consequence of scattering losses caused by these pores.

Therefore, on manufacturing transparent ceramics it is generally recommended to achieve highly dense *and* fine-grained microstructures. This target may appear as not very difficult remembering previous results with fine-grained dense cutting tools, hip implants or ceramic armour ceramics. Here, however, an important *quantitative* difference gives rise to a new quality of the challenge to the manufacturer:

- Influence of the grain size

  The *hardness* of Al_2O_3 increases from grain sizes of 5 μm down to 0.5 μm because of an increasing limitation of the mobility of the elements of microplastic deformation (dislocations and twins); this effect is slightly different in ground and in polished surfaces (due to different frequencies of machining-induced dislocations and twins).[14] In the sub-μm range, however, this influence of grain size *decreases* because of a growing (and counter-acting) influence of the network of grain boundaries (such that real nanomaterials exhibit a decreasing resistance to microplasticity[15]).

  Light transmission through Al_2O_3, however, increases in the sub-μm range in a way that a grain size difference of, e.g. 0.6 or 0.4 μm is of outstanding importance.[1,2]

- Influence of residual porosity

  Obviously, high *mechanical* parameters of Al_2O_3 will not tolerate percents of porosity, but *last tenths* of a percent of porosity remain without significant effect. Therefore, traditional "high tech" ceramics (e.g. for hip implants or cutting tools) are regarded as "dense" when their relative density is, e.g. 99.7%.

  On the other hand, the increase of the real in-line transmission (which governs *transparency*!) just *starts* at residual porosities <0.1–0.2%, and *last hundredths* of a percent of porosity need to be eliminated for obtaining clear transparency.[2]

The need to eliminate last pores is likewise imperative in glasses as in single or polycrystalline transparent materials. However, this technological challenge is much harder when it has to be achieved with pure solid state sintering[d] and at a minimum of grain growth, i.e. at low temperatures. With all these difficulties it is obvious that transparency needs very special, optimized sintering regimes. The most common approach today is pressureless pre-sintering up to closed porosity followed by hot-isostatic post-densification (hot-isostatic pressing, HIP).[1] Other approaches like microwave and millimetre wave sintering[16–18] or spark plasma sintering (SPS[19]) may provide similar results (until present, however, without *improvements* of dense microstructures and their properties[20]) but are often limited to bodies with simple shape (e.g. discs).

[d] Because of optical homogeneity transparent ceramics have to be single-phase materials that cannot be sintered with an additive of several percents of a *liquid* phase.

How ever important—the development and application of an optimized sintering approach is *not the key* to a high transparency: even the most advanced HIP regime will not provide transparent components without (i) selection of the *right raw powder* together with (ii) application of a very special, *defect avoiding processing*.[21] These two issues shall, therefore, be discussed in more detail.

Obviously, with solid state sintering a small particle size is a must regarding the need of an extremely high sintering activity for eliminating *last hundredths* of a percent of porosity. Therefore, it appears practical to look first for the most fine-grained available nanopowder. Fig. 9 shows, however, that this would be a fundamental mistake born by a misunderstanding of the different issues of the performance of *one individual* nanoparticle and the behaviour of the *community* of a very large number of particles:

- The sintering activity of single particles (= the ability of achieving a high final density at low temperature, i.e. with least grain growth) increases with smaller size D because of the increasing surface curvature and shorter distances. On the other hand, the sintering activity of the *macroscopic community* of all particles decreases when the homogeneity H of their mutual arrangement deteriorates[22] (Fig. 9, left).
- However, on processing the surface curvature of finer particles gives rise to stronger aggregation. Thus, the two influences D and H are not independent of each other, and the homogeneity deteriorates with smaller particle sizes (trajectory in central Fig. 9).
- Therefore, the sintering activity S has to be addressed *along this trajectory* $H(D)$ (central diagram of Fig. 9). With the homogeneity $H(D)$ and the particle size D situated on opposite sides of the fraction of $S \sim H(D)^a/D^b$, the sintering activity S is low for large particles, increases for finer powders, and will at very small D depend on the functional character of $H(D)$. Experience shows that S runs through a maximum and decreases at very small D because the homogeneity $H(D)$ exhibits very low values at small finite D.

Thus, Fig. 9 shows that a community of nanoparticles does not at all exhibit a high sintering activity *per se*. Instead, fine-grained powders improve the sintering activity down to some limiting particle size only, e.g. on reducing the particle size from 0.5 to 0.2 μm. The transition to nanoscale sizes will, without special means, *deteriorate* the sintering performance—a fact with multiple evidence by the published body of experience[23,24] but misunderstood frequently as an insufficient degree of optimization.

The path to reach a maximum of sintering activity is demonstrated by the right part of Fig. 9: advanced processing has to improve the *homogeneity* of particle coordination in a way that the position of the maximum is shifted to smaller particle sizes.

Quite naturally, different processing technologies approach this objective of most homogeneous particle coordination in the green bodies differently well:

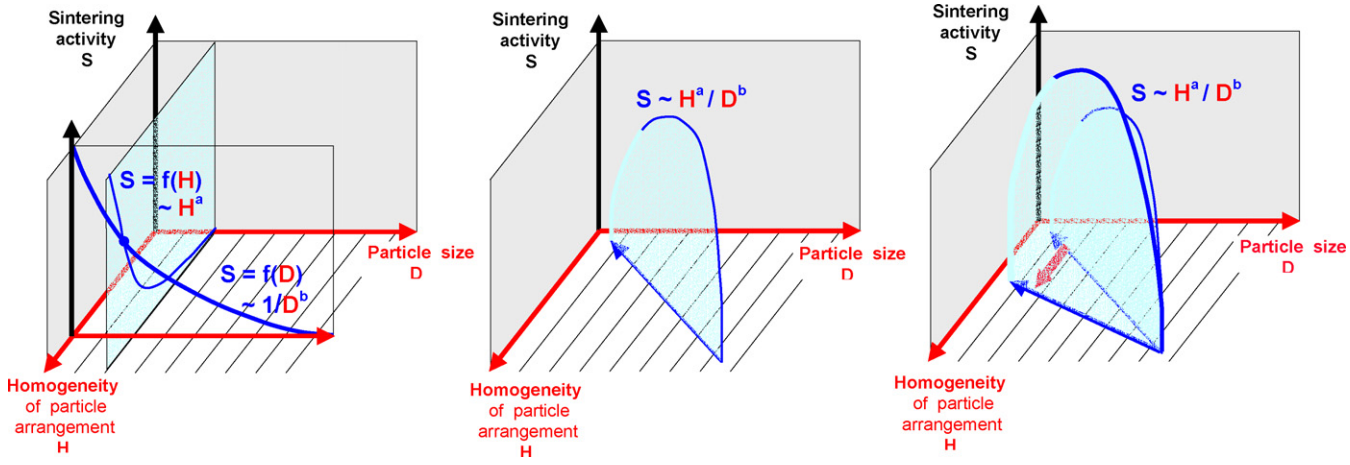

Fig. 9. Influences of (i) particle size D and (ii) homogeneity H of particle arrangement on the "sintering activity" S of the community of all particles. The explanation is that the advantage of short diffusion paths in nanotechnology holds only as far as the particles are homogeneously coordinated, whereas typical aggregation of nanoparticles *increases* the distances between the agglomerates.

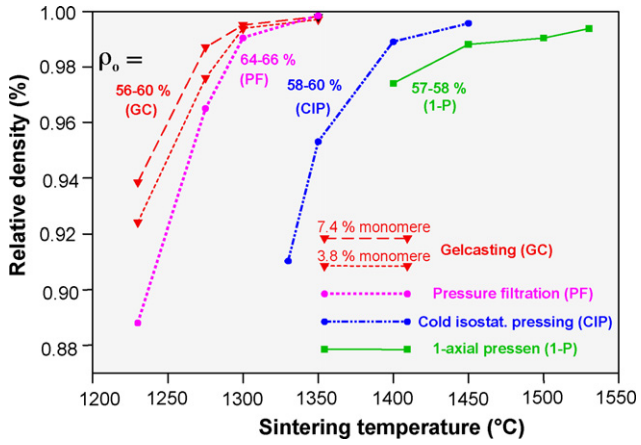

Fig. 10. Sintering of alumina bodies made from *one* 150 nm powder by different processing.[26,27]

- On *pressing*, particles are shielded by the surrounding material, and the externally applied pressure is not able to transfer an individual, small particle into a locally specific, optimum position within the three-dimensional array of its neighbours.
- On *casting*, however, a high mobility can be attributed to each individual particle facilitating its transfer to an optimum position, driven by electrokinetic interaction with the neighbours.

In fact, real profit arises from this option only if the casting approach meets an essential technological prerequisite: the slurries have to associate a *minimum of viscosity* (for perfect de-gassing) with *highest solid contents* (providing a high green density).

Recent investigations have provided experimental evidence of the close, governed by technology, correlation of homogeneity (described on a quantitative basis by the pore size distribution of the green bodies), reduced sintering temperature (for achieving highest densities), and a minimum of grain growth.[25] As an example, Fig. 10 shows the resulting sintering behaviour of bodies shaped from a 150 nm alumina powder: independent of slightly different green densities (ρ_0) there is a clear ranking of the temperatures of pressureless sintering in air which are reduced by defect-avoiding casting by several hundred centigrades. Thus, defect-free shaping turns out as a most important tool for sintering microstructures with high-

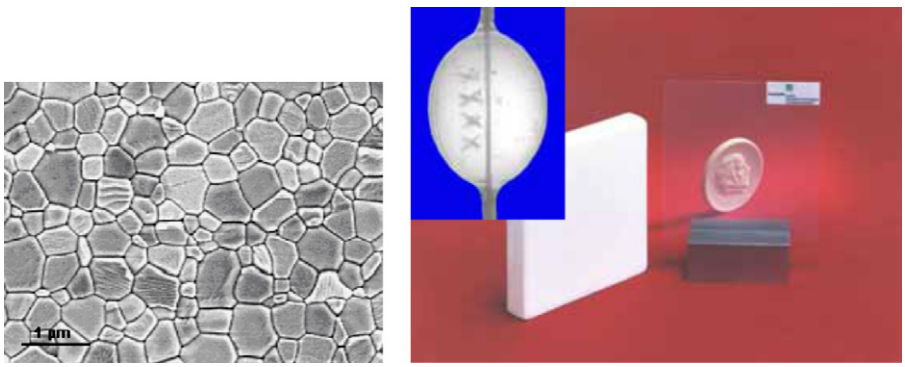

Fig. 11. Opaque and transparent sintered Al_2O_3 of *identical* purity (99.95%), grain size (0.5 μm), hardness HV10 = 21 GPa and 4-point bending strength (600–700 MPa). The one difference is a porosity of ~0.3% in the white but <0.03% in the transparent ceramic (as a demonstration of transparency, the hollow body shows a black wire along the axis and has got an *XXXX* marker on the back). The real in-line transmission of the 0.8 mm thick window is about 60% (=70% of theoretical maximum) at 640 nm wavelength. All bodies from the 150 nm powder used for the study of Fig. 10.

est density at a temperature low enough to minimize grain growth.

Fig. 11 shows the result of combining gelcasting of a 150 nm alumina powder[26,27] with pressureless pre-sintering and subsequent hot-isostatic pressing (HIP). Transparent components of sintered Al_2O_3 are obtained with outstanding mechanical parameters, both as plane windows or – by flexible casting – as hollow envelopes (e.g. for discharge lamps).

The transmission through a birefringent material as alumina with its multiple scattering mechanisms (Fig. 4) is most sensible to negative influences of small imperfections and is, therefore, used here as an example of investigation where the differences between technological approaches are displayed most readily by the resulting optical properties. However, it was outlined above (Figs. 3 and 4) that because of birefringent scattering losses these non-cubic ceramics will hardly exceed a transmission of RIT ≈ 70% over a thin thickness of 1 mm—with the consequence of a transition to a translucent only appearance at larger thickness (Fig. 3). Therefore, fully transparent components with no (or slight) thickness effect can be expected on the basis of cubic materials only.

4. Special focus: cubic transparent ceramics

Without birefringence, ceramics with cubic crystal lattices are not subject to this type of scattering losses and are obvious candidates for transmissions close to the theoretical limit. The manufacture of products is, however, complicated because even for apparently "common" materials like ZrO_2, Y–Al garnet (YAG) or Mg–Al spinel the offer of sufficiently pure commercial raw powders is dramatically smaller than known for alumina. Despite these difficulties, the following cubic sintered ceramics have attracted considerable interest for structural applications.

4.1.1. Aluminum oxynitride ("AlON").

The real composition of this material is close to $9Al_2O_3{\cdot}4AlN$ (width of the range of homogeneity ~10 mol%). In fact, it is cubic γ-Al_2O_3 (spinel structure) with an optimum of about 5 wt% nitrogen.[28] Surmet Ceramics Co., USA is a manufacturer of a high-purity AlON powder[e] (preferentially for own use) and of transparent components made thereof (former manufacturer and development over 20 years: Raytheon[29]). Grain sizes are extremely coarse (250–300 μm) but the material associates a high transmission close to the theoretical limit with the highest hardness known until present for commercial transparent ceramics (HV10 ≈ 15 GPa[f]—what is, however, significantly inferior to HV10 ≈ 21 GPa of transparent sub-μm alumina, Fig. 11).

4.1.2. Mg–Al spinel ($MgO{\cdot}Al_2O_3$)

Mg–Al spinel is another relatively hard cubic transparent ceramic. A commercial manufacturer (compared with AlON on a more exploratory level) is TDA Research Inc., Arvada, CO, USA in cooperation with TA&T, Annapolis, MD, USA,[11,12] and parallel efforts have been reported for Surmet, Mitsubishi (Japan) and others. Only *coarse* microstructures >50 μm with a lower macrohardness of about 12 GPa (see footnote 6) are available,[13] but apparently a really high transmission >80% is obtained with still larger grain sizes of 200–300 μm.[10]

Alternatively, IKTS Dresden/Germany has shown that experiences with defect-free approaches used previously for transparent alumina can be transferred to an advanced processing of spinel powders with about 100 nm particle size. By this means, sintering was enabled at *lower temperatures* resulting in fine-grained sub-μm spinel microstructures (Fig. 12). As a consequence, a transmission close to the theoretical limit (→ no thickness effect—cp., Fig. 2) was associated with a high hardness of HV10 ≈ 15 GPa.

4.1.3. Yttrium oxide (Y_2O_3)

Sintered yttria is rather expensive and subject of few investigations which did not reveal transmission results or mechanical data that could favourably compete with the spinel or AlON grades addressed above. Fine-grained microstructures with grain sizes of about 1 μm were obtained from commercial and laboratory powders with particle sizes between 0.2 and 1 μm by HIP at about 1350 °C.[30] After processing of powders in the range of 60–100 nm, however, a much higher HIP temperature of 1625 °C had to be applied, and the grain size increased to 50 μm.[31]

4.1.4. Y–Al garnet ("YAG"—$1.5Y_2O_3{\cdot}2.5Al_2O_3$)

Three stable phases exist in the Y_2O_3–Al_2O_3 system: an orthorhombic perowskite $YAlO_3$ ("YAP") with an Y/Al ratio 1:1, an alumina-rich cubic garnet $Y_3Al_5O_{12}$ ("YAG"), and an yttria-rich monoclinic phase with composition $Y_4Al_2O_9$ ("YAM"). Sintered YAG ceramics were developed to substitute lanthanide doped single crystals which are a key component in laser devices but where it is difficult to incorporate larger cations (Ce, Pr, Nd, etc.) at high concentrations. Therefore, extended doping is one of the targets of new transparent YAG ceramics.[32] The investigations are of outstanding technological importance since these ceramics are the first example where extremely high optical parameters (least scattering and absorptions losses associated with an extreme homogeneity over the macroscopic volume) were achieved for thicknesses in the centimetre range.

Powders with crystallite size of about 70 nm were sintered and HIP-ed at about 1600–1700 °C resulting in grain sizes of about 2 μm.[33,34] Based on a special powder synthesis[35] with slip-casting and vacuum-sintering,[36] Konoshima (Japan) has become a leading manufacturer of high-grade YAG ceramics.[37] Compared with single crystalline YAG, the transparent *ceramic* YAG exhibits similar low light scattering losses but enables superior doping profiles and larger rod-size capabilities.

More intense sintering gives rise to more grain growth (grain size ~ 10 μm) but reduces the residual porosity to as low as 10^{-4}%.[36] This extreme level is important when scattering losses

[e] Particle size about 0.5 μm.

[f] Higher hardness values refer to *micro*hardness measurements.

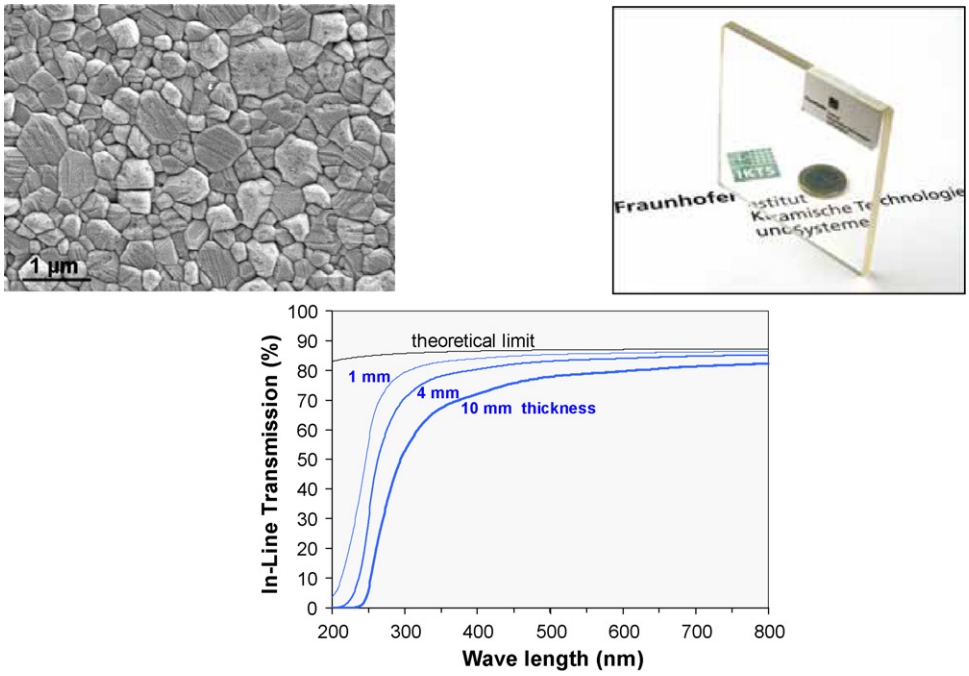

Fig. 12. Transparent sub-μm spinel (grain size 0.42 μm) from a powder with particle size ~100 nm. Small thickness effect in the visible range because of a transmission close to theoretical limit. Macrohardness HV10—15 GPa, 4-point bending strength about 200 MPa.

have to be minimized for the manufacture of *thick* laser components.

4.1.5. Cubic sintered zirconia (ZrO_2, Fig. 13)

Cubic zirconia is not among the very strong and hard ceramics, and its high refractive index near 2.2 is similar to some perowskites.[38] These may be reasons why few investigations have been published on sintered (polycrystalline) transparent ZrO_2 and why the best published transmission data are below the level reported for sintered Mg–Al spinel or AlON.

Single crystals of cubic zirconia are, however, important as artificial gemstones. Their high refractive index gives rise to a high degree of brilliance that comes close to diamonds. In the future the flexibility of *powder technology* in producing more complex shapes may stimulate the substitution of zirconia single crystals by *sintered* transparent decorative and optical products.

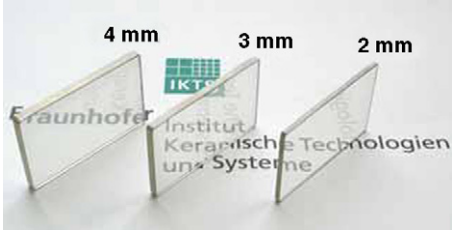

Fig. 13. Cubic sintered ZrO_2 (IKTS Dresden). At λ = 640 nm the real in-line transmission of these windows is 65% (2 mm thickness), 59% (3 mm), and 57% (4 mm), respectively (recalculated for a same thickness of 0.8 mm as in Fig. 11 above (Al_2O_3), this is a transmission of 0.94 of the theoretical limit). The hardness HV10 = 13 GPa is equivalent to the upper limit of zirconia ceramics.

5. Fields of development and application

5.1. Applications powered by transparency–hardness–strength: ceramic armour, dental ceramics, ceramic tools

This special combination of properties limits the selection to few materials: AlON, spinel, and Al_2O_3 ceramics. Ranking will depend on which is the priority parameter.

5.1.1. Ceramic armour

Transparent armour for civil as for military use is one of the most important fields of transparent ceramic development today. The materials have to exhibit clear transparency at several millimetres thickness. It is hard to imagine that sintered alumina will ever match this request. Most potential candidates are, therefore, AlON and spinel.

On the other hand, recent investigations show that, probably, there is no need to focus on the high hardness of Al_2O_3 since new grades of fine-grained sintered spinel exhibit a similarly high ballistic strength as the best sub-μm alumina—outperforming even sapphire (hard core 7.62 mm × 51 AP ammunition, 850 m/s).[39,40] More details are provided by a number of special contributions to this volume.

5.1.2. Orthodontic appliances, future ceramic tools with integrated radiation sensors

Applications which can tolerate a lower transmission but need a higher strength and hardness are bound to sintered corundum (e.g. translucent ceramic brackets[41]). Eventually, future tools for temperature sensible manufacturing (high-speed dry turning of hardened steel, milling of wood-based chip

boards, etc.) will also prefer sub-μm grades of this material.

5.2. Applications associating transparency with thermal/chemical stability: lighting, IR emitters, solar energy

5.2.1. Lighting

Repeated trials to develop "fully transparent" (= cubic) ceramics which stand the highly corrosive high-temperature atmospheres in discharge lamps (e.g. using special grades of Konoshima's transparent sintered garnets for lamps manufactured by Toto/Japan[42]) were not successful. Today these envelopes find application only in lamps for diagnostic purposes where the transparent body facilitates the analysis of the arc. Therefore, no real option that could compete with alumina is known at present.

For several decades *coarse*-grained *translucent* polycrystalline alumina ceramics (PCA, Fig. 4) sintered in hydrogen at 1800–1900 °C have been used as envelopes in discharge lamps (high intensity discharge lamps, HID). The orange colour of high-pressure sodium (HPS) lamps is shifted towards a more whitish appearance when the pressure is increased from approximately 0.15 to 0.40 bar (→colour rendering index CRI ≈ 22). An improved "white" light (→CRI ≈ 80–90) is emitted by metal halide lamps (ceramic discharge metal halide lamps, CDM) introduced by Philips in 1994. These lamps run at a temperature close to 1200 °C—what makes (together with the highly corrosive atmosphere) Al_2O_3 almost irreplaceable as an envelope of outstanding chemical resistance.

The high amount of scattered light from translucent envelopes is not a problem for common lighting application whereas *projection* lamps need transparent materials. HID lamps use silica glass or quartz, but these materials are not sufficiently resistant at the high temperatures and with the corrosive atmosphere of the high-CRI metal halide lamps. Sapphire (single crystalline Al_2O_3) is used for few special lamps but for common applications it is neither sufficiently flexible in shaping nor on a right level of costs.

These needs have promoted the idea to develop *transparent* sintered (polycrystalline) Al_2O_3 discharge envelopes for white-emitting high power metal halide lamps.[1,2] The degree of transparency of polished sub-μm alumina was demonstrated by Fig. 11. It was shown that compared with traditional coarse-grained PCA envelopes this new grade also exhibits a much higher strength (300–400 → 600–700 MPa).

Fig. 14 shows the test of a transparent sub-μm alumina envelope manufactured by gelcasting (same ceramic as in Fig. 11). With this material a first demonstrator was designed and tested with a power of 400 W (which is to be compared with a maximum of about 100 W of previous metal halide lamps).

5.2.2. Infrared emitters

Fast medium-wave infrared heating technology has been introduced into a number of manufacturing processes where large amounts of energy are transferred in a short time, e.g. for heating up small or complex work pieces very quickly. Accordingly, heating and drying can be integrated with finishing operations. Perfectly matched infrared emitters can allow overall energy savings of up to 50%. In the digital printing/narrow web industry the use of advanced IR emitters has dramatically improved the production capacity while reducing electrical consumption in sheetfed offset printing.

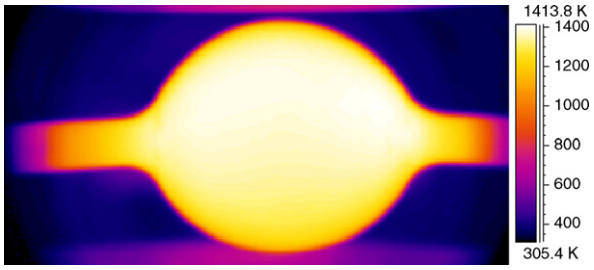

Fig. 14. Thermal photography (false colour) of a burning 400 W CDM lamp with a maximum temperature of about 1150 °C.[43] Sub-μm alumina envelope by IKTS Dresden, lamp demonstrator and test by Philips, Eindhoven.

Today such IR emitters are fabricated with glass envelopes. With the demonstrated general applicability of transparent sintered sub-μm Al_2O_3 for discharge lamps running at very high temperatures (Fig. 14) and with its almost theoretical transmission in the IR range (Fig. 5) a future use of these ceramics for IR heating appears possible as well.

5.2.3. Solar energy

The solar field of a parabolic trough plant consists of long parallel rows of trough-like mirrors which focus the sun energy on a double-wall glassy absorber pipe[g] located along the focal line of the mirrors. A heat transfer fluid (typically an oil) circulating through the pipes is heated to about 400 °C and pumped to a power block where it passes a heat exchanger that generates steam which drives a conventional turbine. There is a design where both tubes are made of glass, but other constructions work without light transmittance *into* the inner absorber pipe which is made of a metallic alloy.

Remembering the high temperatures that can be obtained with focused sun light it is challenging to think about future solutions which may use heat transfer media with a higher temperature >500 °C when the absorber consists of a temperature-resistant transparent ceramic. Such design would enable direct radiation heating of the transfer medium to much higher temperatures than known from the double-wall glass tubes.

5.3. Applications with emphasis to special optical properties: lasers, lenses, decorative products

5.3.1. Ceramics for lasers and for decorative applications

There is one common feature of the rather different fields of laser ceramics and ceramics for decorative art (e.g. gemstones): as outlined above, polycrystalline garnet ceramics are

[g] The double-wall construction of two tubes isolates the inner pipe (with the heat transfer fluid) in order to avoid energy losses by radiation.

Fig. 15. Transparent sintered corundum (α-Al_2O_3) with colours that cover the visible spectrum.

developed because their grain boundaries offer space (on an atomistic scale) to introduce more and larger doping species than can be introduced into the crystal lattice by solid solution only (remember that transparent ceramics have to avoid even small amounts [>0.1%] of second phases to keep scattering losses low).

Fig. 15 is a direct demonstration of this effect applied to artificial corundum gems. As in laser ceramics, the choice of additives (and, thus, of colours) is tremendously widened by the sintered polycrystals manufactured by powder technological approaches[44] whereas in single crystals known colours are limited to red (Cr → ruby) and a light blue (Ti → sapphire) because of the low solubility of most elements in the corundum lattice.

Associated with the ease of shaping when ceramics are manufactured by casting a recent patent application[45] issued by a Swiss company has adopted gelcasting from a previous patent[27] (in the special approach that gives *transparent* alumina[1]) for manufacturing transparent watch housings. Another manufacturer of luxury watches commercially offers a model where parts of the housing consist of a transparent or translucent Al_2O_3 ("...a very expensive material and extremely hard to work with... This very time-consuming process allows us to manufacture only a handful of Mysteriums a week... This is what makes this ... Watch so exclusive").[46]

These new ceramics have to be distinguished from chromium-doped coloured Al_2O_3 *single crystals* (rubies) which are used for decades in the traditional manufacture of higher grade mechanical watches (bearings for the wheel trains, high wear parts such as escape lever and impulse jewel).

Brilliance is increased by a high *refractive index*, and this is the reason why cubic zirconia *single crystals* became famous as an inexpensive substitute of diamond (without reproducing, of course, the extreme hardness of diamond: cubic ZrO_2 is one of the "softest" ceramic materials). *Sintered* fine-grained ceramics, however, exhibit an increased hardness compared with the single crystals. Therefore and with the easy shaping of *sintered* products and their unique colour options, significant future profit can be expected from a commercialization of polycrystalline sintered grades of zirconia (Fig. 13).

5.3.2. Optical components for different wavelengths

Markets for digital cameras and mobile phones with optic equipment are increasing rapidly. Frequently, a compact and small design of the lens systems is imperative for use and gives rise to the search for new transparent materials with high refractive index and high Abbé number. Optical glasses are limited to $n = 1.5–1.85$ but higher values are known for a number of crystalline ceramics that also exhibit a higher scratch and impact resistance. For example, a first camera with a ceramic lens (a cubic perowskite) was presented by the Casio company in 2004 (Fig. 16). Such materials have to be free of any birefringence (what excludes many single crystals). The lens in Fig. 16 consists of $Ba\{(Sn_uZr_{1-u})_xMg_yTa_z\}_vO_w$ with a refractive index (at visible light) of 2.1, developed originally for use as a wave guide (micro- and millimetre waves).[38] It is not clear, however, whether on a long such complex materials will successfully compete on the market with more simple ceramics as, e.g. cubic zirconia (Fig. 13).

Additional challenges arise when optical components have to be designed for use with extremely short or long wavelengths where absorption becomes a serious issue. For example, UV transparent materials have attracted considerable interest as a key issue of the microelectronic chip industry. Microlithography projects a pattern from a photo-mask through an optical system to create IC chips, and their increasing miniaturisation requires more and more tiny "tools" in the form of shorter ultraviolet laser light.

At present, this development has come to a critical stage because most transparent materials exhibit a sharp absorption edge in the UV range: there are no amorphous (glass) and very few crystalline materials which at, e.g. 193 nm associate a suf-

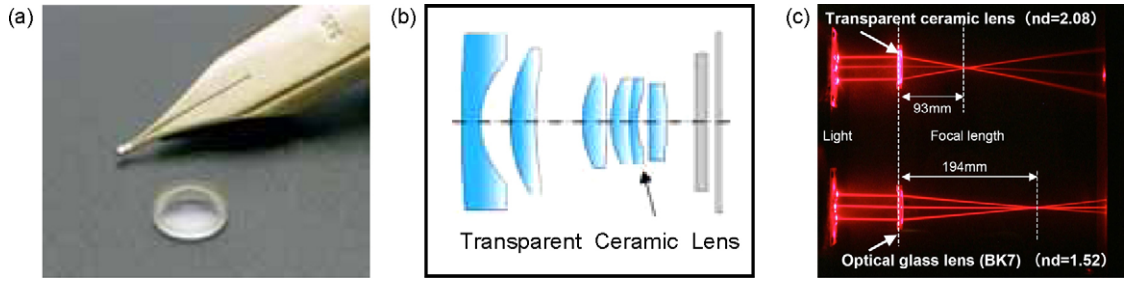

Fig. 16. Ceramic lens manufactured by CASIO from a transparent ceramic LUMICERA™ (Murata[38]). Figure (c) illustrates the smaller focus obtained by the ceramic material compared with glass. Photos by world.casio.com.

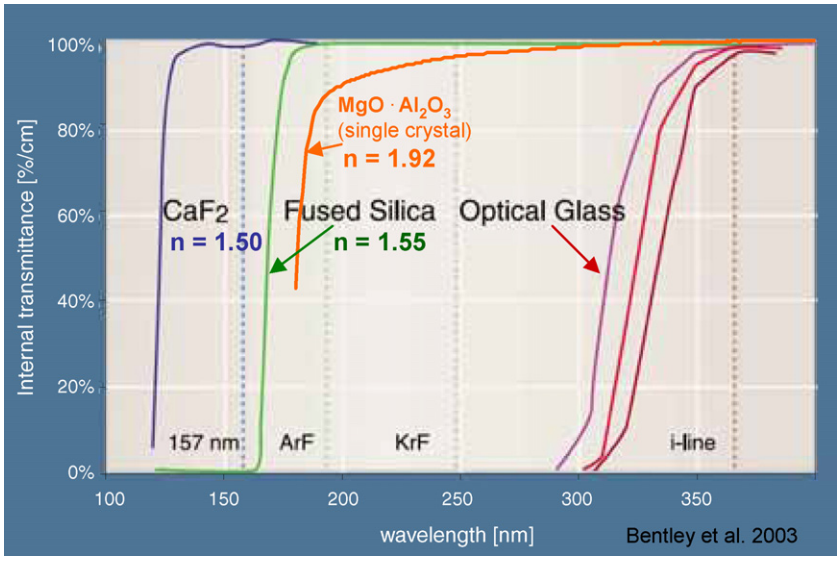

Fig. 17. Wavelengths of UV lasers and wavelength dependent UV transmission of glass and fused silica (quartz) in comparison with Ca–fluoride[47] and single crystalline Mg–Al spinel.[48]

ficiently *high transmission* (Fig. 17) with a *high* (depending on the wavelength) *refractive index* (Fig. 18). Magnesia–alumina spinel is one of few candidates whereas sintered alumina does not exhibit enough transmission at short wavelengths and exhibits, as also sapphire, an absorption edge at about 200–250 nm (Fig. 5).

Unfortunately, the use of *single crystalline* spinel is disabled since the cubic crystals exhibit an inherent birefringence (IBR) at short UV wavelengths.[49] For single crystalline Mg–Al spinel the inherent birefringence is still small at 365 nm (3.6 nm/cm) but increases to 16 nm/cm at 254 nm and to >50 nm/cm at 193 nm.[48]

This effect is known since Lorentz (1878). At very short wavelengths the elementary cell cannot be addressed as a continuum, and wave propagation proceeds slightly different along the edge of the cube and in diagonal direction. In fact, 200 nm wavelength still are much larger than the elementary cell of spinel (∼1 nm), and for decades the limited size of inherent birefringence was technically irrelevant. With the extreme requirements of advanced microlithography, however, the effect cannot be neglected and makes the use of *single crystalline* spinel improbable for this application.[48]

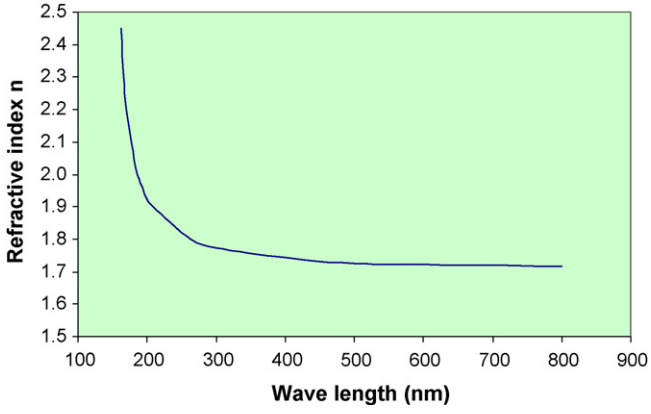

Fig. 18. Strong increase of refractive index at short-UV wavelengths. Example: single crystalline spinel.[48]

Polycrystalline fine-grained (*sintered*) spinel (Fig. 12), however, with its arbitrary orientation of small crystallites is optically completely *isotropic*. In the visible range it exhibits a similar transmission (Fig. 12) as the single crystalline material of Fig. 17 with, unfortunately, bigger differences just at the shorter wavelengths. *Whether* this *option* of polycrstalline spinel can contribute to a solution of the extreme requirements of advanced microlithography must turn out in a competition with the development of new *single crystals* (e.g. Y/Sc–Al or Lu–Al garnets, germanate garnets) that are expected to be free of larger IBR.[50]

6. Summary

Wide ranges of different ceramics are investigated currently with most different microstructures for a use as transparent components. Until present, first commercial products are provided by a very limited number of specialised manufactures who are serving niche markets. Technical applications are, therefore, yet rare. However, some of the new ceramics are expected to find increasing use in different fields of engineering, civil life, and defence.

A real breakthrough will need additional support from commercial raw powder supply. This could also smooth the way for these challenging technologies into enterprises of the traditional ceramic industry which presently is involved on rather a low level yet.

Acknowledgements

The present work uses results from investigations at IKTS Dresden that were performed with financial support of the German Ministry of Defence under contracts E/E210/0D008/I1452 and E/E91S/4A299/3F034. Other parts of this work were funded

by an internal project "MMM Tools: Multiscale Materials Modeling" of the Fraunhofer Society.

References

1. Krell, A., Blank, P., Ma, H., Hutzler, T., Van Bruggen, M. and Apetz, R., Transparent sintered corundum with high hardness and strength. *J. Am. Ceram. Soc.*, 2003, **86**(1), 12–18.
2. Apetz, R. and Van Bruggen, M. P. B., Transparent alumina: a light scattering model. *J. Am. Ceram. Soc.*, 2003, **86**(3), 480–486.
3. Yamamoto, H., Mitsuoko, T. and Iio, S., Translucent polycrystalline ceramic and method for making same. Europe Patent Application EP 1 053 983 A2, IPK[7] C04B35/115, 22.11, 2000.
4. Mao, W., Qi, G., Hong, Q. and Xu, D., Objective lens used in multi-wavelength, multi-layer and multi-level optical storage. In *Proceedings of the SPIE on Advanced Optical Storage Technology, vol. 4930*, ed. D. Xu and S. Ogawa, 2002, pp. 489–492.
5. Mollart, T. P., Wort, C. W., Pickles, C. S., McClymont, M. R., Perkins, N. and Lewis, K. L., CVD diamond optical components, multispectral properties, and performance at elevated temperatures. In *Proceedings of the SPIE on Defense and Security Symposium 2001. VII. Window and Dome Technologies and Materials, Orlando [FL], 2001), vol. 4375*, ed. R. W. Tustison, 2001, pp. 180–198.
6. Krell, A., Hutzler, T. and Klimke, J., Physics and technology of transparent ceramic armor: sintered Al_2O_3 vs. cubic materials, Paper No. 14 in (proceedings CD): applied Vehicle Technological *P*anel: Specialists Meeting on "Nanomaterials Technology for Military Vehicle Structural Applications", Granada, Spain, October 3–4, 2005.
7. Krell, A., Baur, G. and Daehne, C., Transparent sintered sub-(m Al2O3 with IR transmissivity equal to sapphire. In *Proceedings of the SPIE on Defense and Security Symposium 2003. VIII. Window and Dome Technologies and Materials, vol. 5078*, 2003, pp. 199–207.
8. Kinataka, Y., Translucent ceramic, process for producing the same, optical part and optical apparatus. Patent application EP 1 810 955 A1, Int. Class. C04B35/00, July 25, 2007.
9. Gazza, G. E. and Dutta, S. K., Hot pressing of ceramic oxides to transparency by heating in isothermal increments. Patent US 3,767,745, Int. Class. IPK[7]C04B35/64, 23.10.1973.
10. Gilde, G., Patel, P., Patterson, P., Blodgett, D., Duncan, D. and Hahn, D., Evaluation of hot pressing and hot isostatic pressing parameters on the optical properties of spinel. *J. Am. Ceram. Soc.*, 2005, **88**(10), 2747–2751.
11. Reimanis, I. E., Kleebe, H.-J., Cook, R. L. and DiGiovanni, A., Transparent spinel fabricated from novel powders: synthesis, microstructure and optical properties. In *Proceedings of the SPIE on Defense and Security Symposium, Orlando (FL), 13.-15.4.2004*, 2004.
12. Cook, R., Kochis, M., Reimanis, I. and Kleebe, H.-J., A new powder production route for transparent spinel windows: powder synthesis and window properties. In *Proceedings of the SPIE on Defence and Security Symposium 2005. IX. Window and Dome Technologies and Materials, Orlando [FL], 28.3.2005), vol. 5786*, ed. R. W. Tustison, 2005, pp. 41–
47.
13. Patel, P. J., Gilde, G. A., Dehmer, P. G. and McCauley, J. W., Transparent armor. *AMPTIAC Newslett.*, 2000, **4**(3), 1–13.
14. Krell, A., Improved hardness and hierarchic influences on wear in submicron sintered alumina. *Mater. Sci. Eng. A*, 1996, **209**(1/2), 156–163.
15. Yip, S., The strongest size. *Nature*, 1998, **391**, 532–533.
16. Cheng, J., Agrawal, D., Zhang, Y., Drawl, B. and Roy, R., Fabricating transparent ceramics by microwave sintering. *Bull. Am. Ceram. Soc.*, 2000, **79**(9), 71–74.
17. Cheng, J., Agrawal, D., Zhang, Y. and Roy, R., Microwave sintering of transparent alumina. *Mater. Lett.*, 2002, **56**(4), 587–592.
18. Link, G. and Thumm, M., Detailed investigations in microwave sintering of ceramics by means of dilatometer. In *Proceedings of the International Workshop Strong Microwaves in Plasmas, vol. 2*, ed. A. G. Litvak, 2002, pp. 719–724.
19. Dobedoe, R. S., West, G. D. and Lewis, M. H., Spark plasma sintering of ceramics. *Bull. Eur. Ceram. Soc.*, 2003, **1**(1), 19–24.
20. Krell, A. and van Bruggen, M. P. B., Comments on "spark plasma sintering of ceramics". *Bull. Eur. Ceram. Soc.*, 2004, **2**(1), 35.
21. Krell, A. and Ma, H.-W., Sintering transparent and other sub-μm alumina: the right powder. *cfi/Ber. Dt. Keram. Ges.*, 2003, **80**(4), E41–E45.
22. Lange, F., Sinterability of agglomerated powders. *J. Am. Ceram. Soc.*, 1984, **67**(2), 83–89.
23. Li, G., Jiang, A. and Zhang, L., Mechanical and fracture properties of nano-Al_2O_3 alumina. *J. Mater. Sci. Lett.*, 1996, **15**(19), 1713–1715.
24. Li, J. G. and Sun, X., Synthesis and sintering behavior of a nanocrystalline α-alumina powder. *Acta mater.*, 2000, **48**(12), 3103–3112.
25. Krell, A. and Klimke, J., Effect of the homogeneity of particle coordination on solid state sintering of transparent alumina. *J. Am. Ceram. Soc.*, 2006, **89**(6), 1985–1992.
26. Krell, A. and Blank, P., Shaping influence on the grain size dependence of strength in dense submicrometre alumina. *J. Eur. Ceram. Soc.*, 1996, **16**(11), 1189–1200.
27. Krell, A. and Blank, P., Al_2O_3-sintermaterial, Verfahren zu seiner Herstellung und Verwendung des Materials. Europ. Patent EP 756 586 B1, Int. Class. IPK[7] C04B35/111, 29.10.1997 (= US 6,066,585, 23.5.2000).
28. Patel, P. J., Gilde, G. and McCauley, J. W., Transient liquid phase reactive sintering of aluminum oxynitride. US Patent 7,045,091 B1, Int. Class. C04B35/10, 16.05.2006.
29. Hartnett, T. M., Gentilman, R. L. and Maguire, E. A., Aluminum oxynitride having improved optical characteristics and method of manufacture. US Patent 4,481,300, Int. Class. IPK[7] C04B35/58, 06.11.1984.
30. Yeheskel, O. and Tevet, O., Elastic moduli of transparent yttria. *J. Am. Ceram. Soc.*, 1999, **82**(1), 136–144.
31. Mouzon, Y., Syntheses of Yb:Y_2O_3 nanoparticles and fabrication of transparent polycrystalline yttria ceramics. Dissertation, Lulea University of Technology, 2005.
32. Feng, T., Shi, J. and Jiang, D., Preparation and optical properties of transparent Eu^{3+}:$Y_3Al_{5(1-x)}Sc_{5x}O_{12}$ ceramics. *J. Am. Ceram. Soc.*, 2006, **89**(5), 1590–1593.
33. Lee, H. D, Mah, T.-I., Parthasarathy, T. A. and Keller, K. A., YAG lasing systems and methods. US Patent Application US 2005/0281302 A1, Int. Class. IPK[7] H01S3/16, 22.12.2005.
34. Li, J.-G, Ikegami, T., Lee, J.-H. and Mori, T., Low-temperature fabrication of transparent yttrium aluminum garnet (YAG) ceramics without additives. *J. Am. Ceram. Soc.*, 2000, **83**(4), 961–963.
35. Matsushita, N., Tsuchiya, N., Nakatsuka, K. and Yanagitani, T., Precipitation and calcination process for yttrium aluminum garnet precursors synthesized by the urea method. *J. Am. Ceram. Soc.*, 1999, **82**(8), 1977–1984.
36. Kumar, G. A., Lu, J., Kaminskii, A. A., Ueda, K.-I., Yagi, H., Yanagitani, T. *et al.*, Spectroscopic and stimulated emission characteristics of Nd^{3+} in transparent YAG ceramics. *IEEE J. Quantum Electron.*, 2004, **40**(6), 747–758.
37. Yagi, H., Transparent YAG ceramics. *Bull. Am. Ceram. Soc.*, 2005, **84**(5), 9.
38. Tanaka, N., Higuchi, Y., Katsube, M. and Sube, M., Transparent ceramic and method for production thereof, and optical element. PCT Patent Application WO 02/49984 A1, Int. Class. IPK[7] C04B35/00, 27.6.2002.
39. Krell, A. and Strassburger, E., Hierarchy of key influences on the ballistic strength of opaque and transparent armor. In *Ceram. Eng. & Sci. Proc. 28 (2007) [5] Advances in Ceramic Armor III*, ed. L. Prokurat Franks. Wiley & Sons, Hoboken, 2007, pp. 45–55.
40. Krell, A., Hutzler, T. and Klimke, J., Transparent armour: Spinel vs. sintered sub-μm Al_2O_3, this volume.
41. Kelly, J. S. and Gille, H. K., Ceramic orthodontic appliance. US Patent 4,954,080, Int. Class. IPK[7] A61C3/00, 04.09.1990.
42. http://www.lightbulbs.booking163.com/Spec%20Sheets/Toto%20YAG70.htm (internet page of Toto Ceramic Co. Ltd.), April 2006.
43. Van Bruggen, M. P. B. and Cnoops, M. P. M., Alumina ceramics in discharge lamps—transforming translucency into transparency. *kgk. Klei. Glas. Keramiek.*, 2004, **25**(1), 14–18.
44. Klimke, J., Krell, A., Hutzler, T, and Blank, P., Farbiges transparentes Korundmaterial mit polycrystallinem sub-μm Gefüge und Verfahren zur

Herstellung von Formkörpern aus diesem Material. German Patent Application DE 10 2004 003 505 A1, Int. Class. C30B29/20, 18.08.2005.
45. Christian, V. and Bach, M., Elément de fermeture ou d'habillage transparent et inrayable pour une montre et montre munie d'un tel élément. Europ. Patent Application EP 1 507 180 A1, Int. Class. IPK[7]G04B37/22, 12.02. 2005.
46. http://www.kriegerwatch.com/ip.asp?op=Mysterium&m=x005000 Collections.
47. Bentley, J., Cadel, S., Hrdina, K., Kohli, J., Linder, M., Price, M. *et al.*, Matter matters—optical materials rise to the microlithography challenge. *Spie's oe Mag.*, 2003, 26–28.
48. Burnett, J. H., Kaplan, S. G., Shirley, E. L., Tompkins, P. J. and Webb, J. E., High-index materials for 193 nm immersion lithography. In *Proceedings of the Optical Microlithography XVIII (Proc. SPIE, vol. 5754)*, ed. B. W. Smith, 2005, pp. 611–621.
49. Burnett, J. H., Levine, Z. H., Shirley, E. L. and Bruning, J. H., Symmetry of spatial-dispersion-induced birefringence and its implications for CaF_2 ultrviolet optics. *J. Microlithogr. Microfabr. Microsyst.*, 2002, **1**(3), 213–224.
50. Burnett, J. H., Kaplan, S. G. and Shirley, E. L., High-index materials for 193 nm immersion lithography. www-presentation of NIST (National Institute of Standards, USA) at http://physics.nist.gov/Divisions/Div842/Gp3/DUVMatChar/high IndexMat.html, 2006.